Molecular Organization in the Pseudo-hexagonal Crystalline Phase of Ethylene−Propylene Copolymers

Odda Ruiz de Ballesteros,[†] Finizia Auriemma,*[,†] Gaetano Guerra,[‡] and Paolo Corradini[†]

Dipartimento di Chimica, Università degli studi di Napoli Federico II, Via Mezzocannone 4, I-80134 Napoli, Italy, and Dipartimento di Chimica, Università di Salerno, I-84081 Baronissi (SA), Italy

Received April 4, 1996; Revised Manuscript Received July 2, 1996[⊗]

ABSTRACT: A detailed X-ray diffraction pattern of an oriented sample of the ethylene−propylene copolymer (75 mol % of ethylene) in the pseudo-hexagonal form is presented. The comparison between the experimental diffraction intensities with the calculated intensities for ordered and disordered pseudo-hexagonal chain aggregates has allowed us to clarify some features of the structure of the pseudo-hexagonal form of the ethylene−propylene copolymers: (i) the methyl groups of the propylene monomeric units are included in the crystalline phase; (ii) the pseudo-hexagonal packing of the nearly *trans*-planar copolymer chains corresponds locally to relative shifts of neighboring chains nearer to those observed in the monoclinic and in the more common orthorhombic form of polyethylene; (iii) the ratio between the integrated intensities of the main peaks on the first layer line and on the equator can be accounted for by conformational disorder, implying a waviness of the nearly *trans*-planar chains and departures from strictly 180° of internal rotation angles in the backbone chains; (iv) some further partial disorder (intermolecular translational along *c* and intermolecular rotational around *c*) should be introduced to account for the broadness of the nonequatorial peaks. A comparison between the presently proposed structure for the pseudo-hexagonal form of the ethylene−propylene copolymer with other disordered structures of homopolymers and copolymers with a hexagonal arrangement of the chain axes is also presented.

1. Introduction

The random introduction of methyl branches along the polyethylene chain causes a decrease of the crystallinity with increasing propylene content, and copolymers with an ethylene content below 60 mol % are essentially amorphous.[1−5] However, it is well established that propylene units enter into the lattice of orthorhombic polyethylene, gradually increasing the disorder in the crystalline phase but leaving substantially unaltered the *trans*-planar conformation of the chains. In fact, the dimension of the *a* axis of the unit cell of polyethylene increases almost proportionally to the propylene content of the copolymer, whereas the *b* and the *c* axes practically retain the dimensions found in polyethylene.[3,6−12] For high propylene content, *a* becomes nearly equal to $b\sqrt{3}$ and hence the unit cell becomes pseudo-hexagonal.[1]

In particular, the X-ray diffraction spectra of a stretched sample with an ethylene content of 75 mol % has been interpreted[1] on the basis of a pseudo-hexagonal unit cell with $a_h = 5.0$ Å and $c = 2.54$ Å, which can be also described as an orthorhombic cell ($a_o = 8.7$ Å, $b = 5.0$ Å, and $c = 2.54$ Å) to be compared with the orthorhombic cell of polyethylene ($a_o = 7.40$ Å, $b = 4.93$ Å, and $c = 2.54$ Å),[13] (the subscript h and o standing for hexagonal and orthorhombic, respectively). It has been also established that the pseudo-hexagonal form is disordered and the long-range positional order in three dimensions is substantially maintained only for the chain axes[1] (that is, for a structural feature which is not point-centered).[14]

In this contribution, the structure of the pseudo-hexagonal form, which is present in stretched samples of ethylene−propylene copolymers, is investigated by X-ray diffraction measurements and Fourier transforms calculations of models. In a first section, the X-ray diffraction pattern of a sample with an ethylene content of 75 mol %, stretched at room temperature with an elongation of 750%, collected with an automatic diffractometer, is presented, thus providing quantitative information relative to the diffraction intensity of the pseudo-hexagonal form. In our knowledge, this kind of information is not present in the literature. In the second section of the paper, a possible structure for the disordered pseudo-hexagonal form is proposed on the basis of semiquantitative comparisons between the experimental diffraction intensity and the calculated Fourier transforms of models consisting of ordered and disordered aggregates of nearly *trans*-planar chains.

2. Experimental Section

The ethylene−propylene copolymer samples were supplied by Montell "Centro Ricerca Giulio Natta" of Ferrara. The comonomer distribution is essentially random. It was obtained with a single-site metallocene based polymerization catalyst, which should behave with good regio- and stereospecificity for the propylene comonomer.[15]

Oriented samples were obtained by stretching at room temperature strips of compression molded sheets 1.35 mm thick. The X-ray diffraction measurements were performed on stretched samples maintained at a fixed elongation.

The X-ray photograph was obtained by using a cylindrical camera with Ni-filtered Cu Kα radiation.

The X-ray diffraction patterns were obtained by using a Nonius automatic CAD4 diffractometer, with Ni-filtered Cu Kα radiation, and were collected always maintaining an equatorial geometry. The measurements have been performed along the reciprocal cylindrical ξ coordinate in the range $0 < \xi < 0.8$ Å^{-1} at intervals of 0.006 Å^{-1}, and for $\zeta = l/c$, with $l = 0$, 1, 2 and $c = 2.54$ Å, corresponding to the chain identity period, and along the meridian (i.e., for $\xi = 0$) in the range $0 < \zeta < 0.9$ Å^{-1} at intervals of 0.006 Å^{-1}.

The Lorentz and polarization (Lp) correction, when used (Figures 2B and 3B), is, according to the diffraction geometry, $\mathrm{Lp} = (1 + \cos^2 2\vartheta)/(\sin 2\vartheta)$.

[†] Università degli studi di Napoli Federico II.
[‡] Università di Salerno.
[⊗] Abstract published in *Advance ACS Abstracts,* August 15, 1996.

S0024-9297(96)00511-6 CCC: $12.00

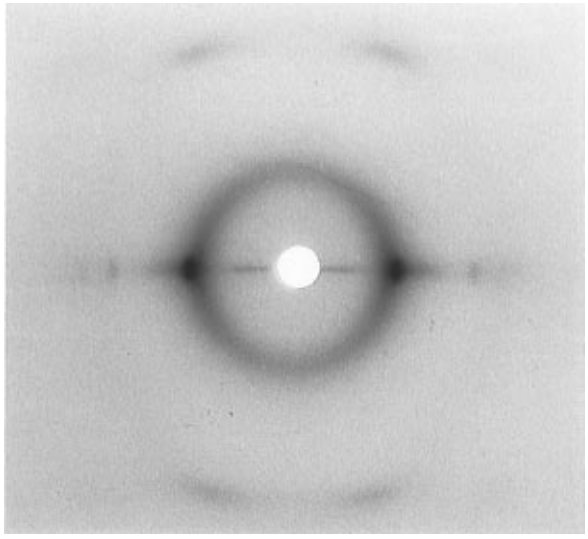

Figure 1. X-ray diffraction pattern, taken with a cylindrical camera (Ni-filtered Cu Kα radiation), of an ethylene−propylene copolymer sample (ethylene content 75 mol %) stretched at room temperature (elongation ratio = 750%).

3. Experimental Results and Discussion

A photographic X-ray diffraction pattern obtained by a cylindrical camera for the copolymer sample at elongation of 750% is shown in Figure 1. Three equatorial reflections are clearly apparent, which correspond to (100), (110), and (200) indexes of a pseudo-hexagonal cell with $a = 4.94$ Å. An amorphous halo partially polarized on the equator is centered at $2\vartheta = 19.5°$. A second very weak halo is centered at 40.5°. The pattern of Figure 1 shows also a layer line, corresponding to a periodicity of 2.54 Å, including a broad intense peak centered at $2\vartheta = 41.5°$ and a second very weak peak at $2\vartheta = 53.5°$.

The diffraction intensities as collected by an automatic diffractometer along the equator and the layer lines with $\zeta = l/c$ (l integer ≤ 2) corresponding to a periodicity of $c = 2.54$ Å are plotted in Figure 2A vs the reciprocal coordinate ξ. The diffraction intensity on the meridian (that is, the intensity at $\xi = 0$ for variable values of ζ) is reported in Figure 3A. The dotted curves in Figures 2A and 3A show the background contributions. The diffraction intensities (I_0), after subtraction of the background and correction by the Lorentz and polarization factors (Lp), are reported, for the layer lines and the meridian, in Figures 2B and 3B, respectively.

In Figures 2B and 3B, the amorphous contribution is indicated by dashed lines. It is apparent from the photographic pattern of Figure 1 that the first halo is in the region of the main equatorial peak whereas the second (less intense) halo is in the region of the 3rd equatorial peak and of the main peak on the first layer line. Moreover, the meridional profile in the range $0.1 < \xi < 0.7$ Å^{-1} (broad halos at $\zeta = 0.21$ Å^{-1} and $\zeta = 0.45$ Å^{-1} in Figure 3B) is essentially due to the above-described amorphous halos.

In summary, the X-ray diffraction pattern of the pseudo-hexagonal phase of the copolymer presents, besides three sharp equatorial reflections, some broad peaks on well-defined layer lines. This indicates that a long-range order is possibly maintained only inside each chain (the backbone conformation remaining nearly *trans*-planar) and in the pseudo-hexagonal arrangement of the chain axes. A substantial intermolecular disorder between neighboring chains is clearly indicated; in particular, as for other disordered polymeric hexagonal phases,[14,16,17] the occurrence of translational disorder along *c*, as well as of rotational disorder around the chain axes, is expected.

The experimental half-height widths of the main equatorial and of the meridional peaks are 0.015 Å^{-1} (along ξ) and 0.010 Å^{-1} (along ζ), respectively. On this basis, the lateral and longitudinal (mean chain length)

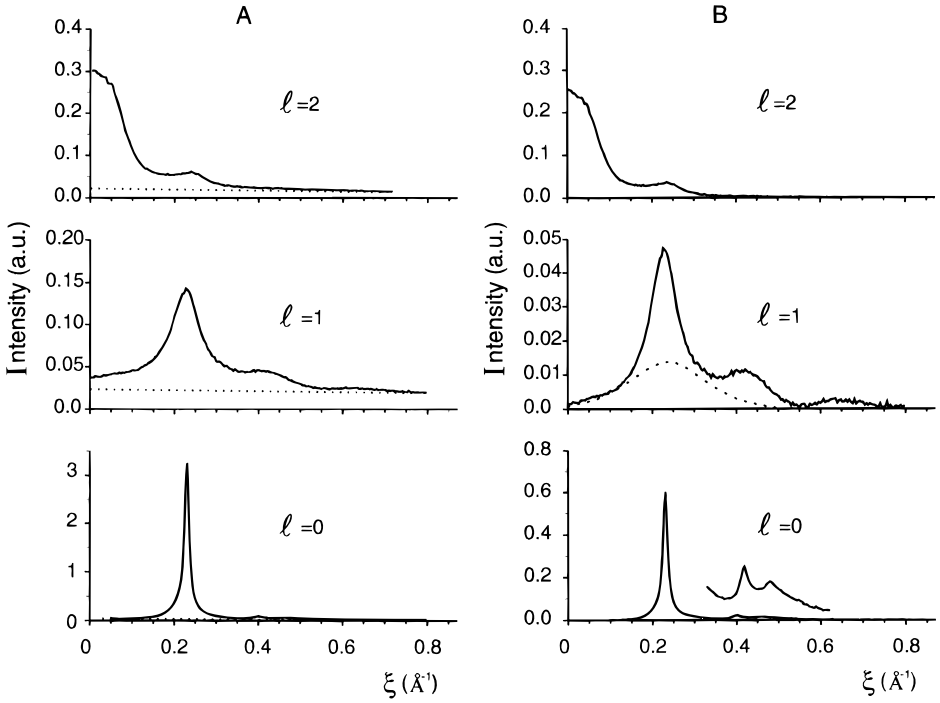

Figure 2. X-ray diffraction profiles (I_0) of the same sample of Figure 1 vs the reciprocal coordinate ξ for the equator and the indicated layer lines (periodicity $c = 2.54$ Å) collected with an automatic diffractometer: (A) experimental (the dotted curves indicate the background contribution); (B) subtracted for the background and corrected by the Lorentz and polarization factor (the dashed curves indicate the amorphous contribution).

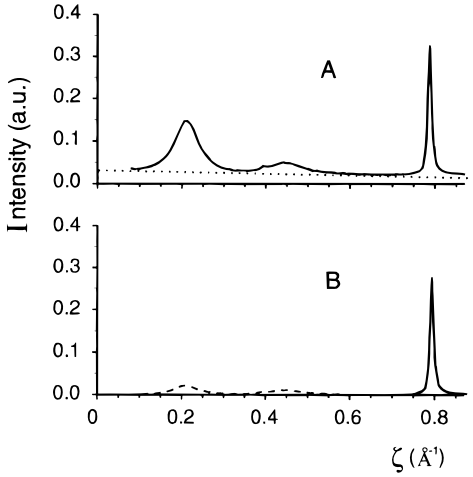

Figure 3. X-ray diffraction intensity (I_0) of the same sample of Figure 1 vs the reciprocal coordinate ζ along the meridian ($\xi = 0$) collected with an automatic diffractometer: (A) experimental (the dotted curve indicates the background contribution); (B) subtracted for the background and corrected by the Lorentz and polarization factor (the dashed curve indicates the amorphous contribution).

dimensions of the structural models used in the forthcoming Fourier transform calculations have been established (see later).

It is apparent from Figure 1 that our copolymer sample is not perfectly oriented along the stretching direction. Indeed, the not perfect parallelism of the chain axes with the drawing direction broadens the diffraction peaks along circles in reciprocal space at 2ϑ constant. The incomplete orientation of the sample should also broaden the intensity distribution of Figure 2 on the layer lines at low ξ values. The effect is sensible for the meridional intensity maximum of the second layer line. Based on these considerations, reasonable estimates of half-height width of the peaks on the first and on the second layer lines along ξ ($w(1)$ and $w(2)$, respectively), as well as of the ratio between the integrated intensities of the main peaks on the first layer line and on the equator ($I(1)/I(0)$) or between the integrated intensities of the mean peaks on the second layer line and on the equator ($I(2)/I(0)$), can be reasonably attempted from the available experimental data. Indeed, $w(1)$ and $I(1)/I(0)$ would be around 0.06 Å^{-1} and to 0.18, respectively, whereas $w(2)$ and $I(2)/I(0)$ would be around 0.11 Å^{-1}and 1.3, respectively.

4. Model Structures for the Trial Calculations

Three limiting ordered models are considered (shown in Figure 4). They all present a long-range order as far as the periodicity along the chain axis (equal to 2.54 Å, the backbone chain being *trans*-planar) and in the hexagonal arrangement of the chain axes (placed at distance equal to 4.94 Å). All the considered limiting ordered models present $b-c$ layers of chains for which the planes of the zig-zag backbones are parallel. Successive chains along the $b-c$ layers have the same quote along z for the models of Figures 4A and 4B, while are shifted by $^1/_2c$ for the models of Figure 4C. The planes of the zig-zag backbones of chains of adjacent layers along a_0 are perpendicular for the model of Figure 4A, while they are parallel for the models of Figures 4B and 4C. The relative orientation of the chains in the models of Figures 4A, 4B, and 4C is analogous to those observed in the orthorhombic[13] and in the monoclinic[18] form of polyethylene and in a triclinic polymorph of long chain paraffins,[19] respectively. Hence, hereafter the models of Figures 4A, 4B, and 4C will be named orthorhombic-like, monoclinic-like, and triclinic-like, respectively. This choice of the limiting models is also based on the calculations of Kitaigorodsky[20] on polyethylene for which only the three energy minima corresponding to the orthorhombic, monoclinic, and triclinic packing models have been found.

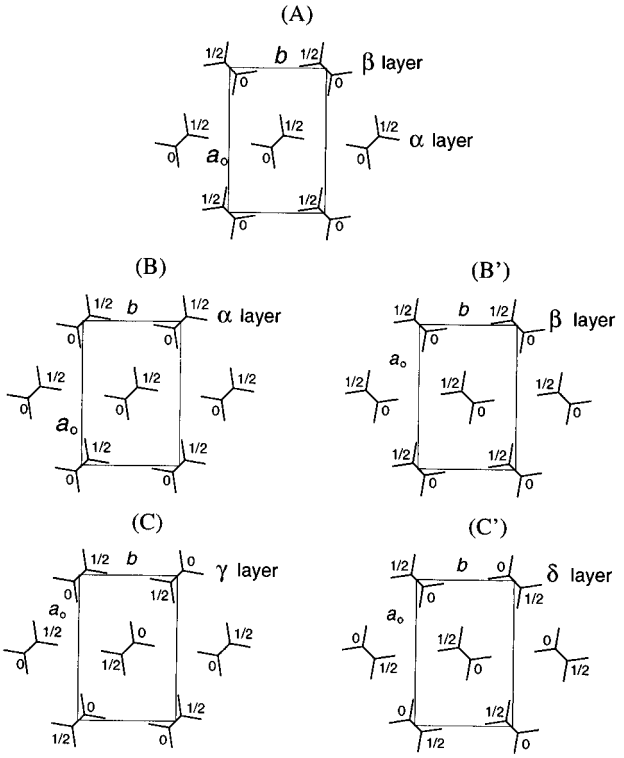

Figure 4. $x-y$ plane projection of the limiting ordered models: (A) orthorhombic-like arrangement; (B) and (B′) monoclinic-like arrangement; (C) and (C′) triclinic-like arrangement. The numbers indicate the fractional z coordinate of the backbone carbon atoms. Greek letters indicate the different kinds of layers.

The trial calculations, which will be reported in this paper, were performed on the (pseudo-hexagonal) limiting ordered models as above, with the following kinds of disorder:

(1) Thermal disorder due to thermal vibrations of atoms. It is treated anisotropically, with the components of the thermal factor parallel and perpendicular to the chain axis (B_ζ and B_ξ, respectively);

(2) Conformational disorder: small displacements from the *trans* state of the backbone dihedral angles (close to the tertiary C atoms), keeping the mean periodicity close to 2.54 Å;

(3) Translational intermolecular disorder along the chain axis;

(4) Rotational intermolecular disorder around the chain axis;

(5) Disorder in the piling of layers of chains (stacking faults).

These kinds of disorder will be introduced separately and/or together, in order to better understand their influence on the calculated diffraction profiles. Due to the disordered nature of the pseudo-hexagonal form of ethylene−propylene copolymer, the comparison between the calculated and the experimental diffraction data may be established only on a semiquantitative basis.

5. Calculation Methods

The square modulus of the structure factor (I), to be compared with the experimental X-ray diffraction (I_0), is calculated according to two methods, depending on the kind of disordered models: method I is used for model structures involving translational, rotational, and conformational disorder, while method II is used for model structures involving stacking faults. In this last case, method II is preferred to method I, since it evaluates in a more straightforward manner the average square modulus of the structure factors for model structures in which the disorder develops along one direction only. We have checked that the two methods give strictly coincident results, when applied to a same model structure.

The bundles of chains considered have global hexagonal (in method I) or rectangular (in method II) shapes. On the basis of the experimental value of the half-height widths of the main meridional (along ζ) and equatorial (along ξ) peaks: the length of each chain in the bundles is fixed equal to 70 Å (28 monomeric units), whereas the lateral size of the hexagonal bundles (distance between two parallel edges) is fixed to nearly 60 Å (corresponding to 127 chains); for method II the number of $b-c$ layers (N) and the number of the chains inside each $b-c$ layer is varied, instead (*vide infra*). In order to reproduce the relative intensities of the three equatorial reflections, in all the calculations the thermal factor B_ξ was fixed equal to 22 Å^2. For the sake of simplicity, B_ζ was set equal to zero, instead.

5.1. Method I. We deal with large bundles of chains in which "paracrystalline disorder" of the kind discussed by Hosemann et al. (ref 21, Chapter IX; see also Tadokoro, ref 22, Chapter 4) is present.

The square modulus of the structure factor (I) cylindrically averaged in the reciprocal space is given by the equation:

$$I = \sum_{K=1}^{M}\sum_{J=1}^{M}\sum_{k=1}^{m}\sum_{j=1}^{m} f^2 J_0(2\pi\xi r_{KkJj}) \times \exp[-2\pi i(z_{Kk} - z_{Jj})] D \sin^2(\pi Cc\zeta)/\sin^2(\pi c\zeta) \times \exp(-2\pi^2\xi^2 u_\xi^2 r_{KJ}/r_{12}) \exp(-2\pi^2\zeta^2 u_\zeta^2 r_{KJ}/r_{12}) \quad (1)$$

The detailed derivation of the eq 1 is reported in ref 23. For our purpose, it is enough to recall that M is the number of the chains in the bundle, m the number of atoms in a monomeric unit, and C the number of monomers in a chain; r_{KkJj} and r_{KJ} are the projections in the $a-b$ plane of the distance between the kth atom in a monomeric unit belonging to Kth chain and the jth atom in a monomeric unit belonging to the Jth chain and of the distance between the axes of the Kth and Jth chain, respectively; the term $J_0(2\pi\xi r_{KkJj})$ is the 0th order Bessel function with the argument given between the parentheses; the factors u_ξ^2 and u_ζ^2 in the exponential terms are the mean square displacements of the coordinates (r and z, respectively) of the centers of gravity of the chains whereas the factor r_{12} is the distance in the $x-y$ plane between the axes of two first neighboring chains; D is the Debye factor $D = \exp(-\xi^2 B_\xi/2) \exp(-\zeta^2 B_\zeta/2)$. The factors $\exp(-2\pi^2\xi^2 u_\xi^2 r_{KJ}/r_{12})$ and $\exp(-2\pi^2\zeta^2 u_\zeta^2 r_{KJ}/r_{12})$ reduce the interference between each couple of chains, the more, the higher is their distance in the $x-y$ plane, and hence correspond to a paracrystalline disorder.

5.2. Method II. This method is used to evaluate the influence on the calculated X-ray diffraction profiles when disorder develops in one dimension only (i.e., in which ordered layers of chains include stacking faults).[24] It is indeed possible to describe the limiting ordered structures of Figure 4 in terms of layers $b-c$ of chains piled along the direction a_0 according to different patterns. The $b-c$ layers are characterized by the repetition along b of parallel chains with translation vector $\mathbf{t_1} = \mathbf{b}$, in Figures 4A, 4B, and 4B′, or $\mathbf{t_2} = \mathbf{b} + \mathbf{c}/2$, in Figures 4C and 4C′. According to whether the zig-zag planes of the backbone chains are inclined by +45° or −45° to the $\mathbf{a_0}$ direction, we distinguish at least four kinds of layers, named α, β, γ and δ in the Figure 4. An orthorhombic-like arrangement (see Figure 4A) is characterized by the regular alternation of layers α and β along a_0, the translation vector among consecutive layers being $\mathbf{s_1} = \mathbf{a_0}/2 + \mathbf{b}/2$. In a monoclinic-like arrangement (see Figures 4B and 4B′), identical $b-c$ layers of chains of kind α (or equivalently β) are piled along a_0, the translation vector between consecutive $b-c$ layers of chains being $\mathbf{s}_1$, the same as before. In a triclinic-like arrangement, identical $b-c$ layers of kind γ (or equivalently δ) follow each other along a_0, the translation vector among consecutive layers being $\mathbf{s_2} = \mathbf{a_0}/2 + \mathbf{b}/2 + \mathbf{c}/2$ for the layers of kind γ, $\mathbf{s}_1$ for the layers of kind δ.

Chart 1. Conditional Probabilities and Possible Translation Vectors among Consecutive $b-c$ Layers Piled along a_0

	$(\alpha)_{i+1}$	$(\beta)_{i+1}$	$(\gamma)_{i+1}$	$(\delta)_{i+1}$
$(\alpha)_i$	p_m, $\mathbf{s_1}$	p_o, $\mathbf{s_1}$	p_{tt}, $\mathbf{s_1}$, $\mathbf{s_2}$	p_{tt}, $\mathbf{s_1}$, $\mathbf{s_2}$
$(\beta)_i$	p_o, $\mathbf{s_1}$	p_m, $\mathbf{s_1}$	p_{tt}, $\mathbf{s_1}$, $\mathbf{s_2}$	p_{tt}, $\mathbf{s_1}$, $\mathbf{s_2}$
$(\gamma)_i$	p'_t, $\mathbf{s_1}$, $\mathbf{s_2}$	p'_t, $\mathbf{s_1}$, $\mathbf{s_2}$	p_t, $\mathbf{s_2}$	-
$(\delta)_i$	p'_t, $\mathbf{s_1}$, $\mathbf{s_2}$	p'_t, $\mathbf{s_1}$, $\mathbf{s_2}$	-	p_t, $\mathbf{s_1}$

The disordered models can be easily described in terms of probability of succession of the various kinds of $b-c$ layers with various translation vectors. Chart 1 summarizes the probabilities and the possible translation vectors between consecutive layers. p_m is the conditional probability that, given that the ith $b-c$ layer is of kind α (or β), the (i+1)th layer is of the same kind α (β), realizing locally a monoclinic-like (strictly hexagonal) sequence; p_o is the conditional probability that, given that the ith $b-c$ layer is of kind α (or β), the (i+1)-th layer is of the kind β (α), realizing locally an orthorhombic-like arrangement; p_{tt} is the conditional probability that, given that the ith $b-c$ layer is of kind α (or β), the (i+1)th layer is of the kind γ or δ; p_t is the conditional probability that, given that the ith $b-c$ layer is of kind γ (or δ), the (i+1)th layer is of the same kind γ (δ), realizing locally a triclinic-like arrangement ; p'_t is the conditional probability that, given that the ith $b-c$ layer is of kind γ (or δ), the (i+1)th layer is of the kind α or β.

Of course, the following relationship should be valid among the conditional probabilities:

$$p_m + p_o + 4p_{tt} = 1 \qquad 0 \le p_o, p_h \le 1; 0 \le p_{tt} \le 0.25 \quad (2)$$

$$p_t + 4p'_t = 1 \qquad 0 \le p_t, p_t \le 1; 0 \le p'_t \le 0.25$$

and, with f_α, f_β, f_γ, and f_δ the *a priori* probabilities of occurrence of layers of the kind α, β, γ, and δ, respectively, the following relationships are also valid:

$$f_\alpha = f_\beta = \frac{2(1 - p_t)}{16p_{tt} + 4 - 4p_t} \quad (3)$$

$$f_\gamma = f_\delta = \frac{2(1 - 4f_\alpha)}{4}$$

Following the method given by Allegra,[24] the calculation of the square modulus of the structure factor, I, is given by:

$$I = N\mathbf{FBF}^* + \mathbf{F}[\sum_{j=1}^{N-1}(N-j)\mathbf{BQ}^j + \sum_{j=1}^{N-1}(N-j)\mathbf{BQ}^{*j}]\mathbf{F}^* \quad (4)$$

N is the number of $b-c$ layers piled along a_0, $\mathbf{F}$ is the row vector whose elements are the structure factors of the various kinds of $b-c$ layers $|F_\alpha\ F_\beta\ F_\gamma\ F_\delta|$, $\mathbf{F}^*$ is the column vector of the corresponding complex conjugates, and $\mathbf{B}$ is the diagonal matrix:

$$\mathbf{B} = \begin{vmatrix} f_\alpha & 0 & 0 & 0 \\ 0 & f_\beta & 0 & 0 \\ 0 & 0 & f_\gamma & 0 \\ 0 & 0 & 0 & f_\delta \end{vmatrix} \quad (5)$$

$\mathbf{Q}$ is the matrix shown in eq 6. $\mathbf{Q}^*$ is the corresponding complex conjugate and $\mathbf{q}$ the reciprocal scattering vector $2(\sin\vartheta)/\lambda$ multiplied by $2\pi i$. Equation 3, multiplied by the Debye factor given above, gives the calculated intensity I, to be compared with I_0.

6. Results of the Calculations

6.1. Preliminary Calculations on Limiting Ordered Models. For the sake of simplicity, the calculations reported in this section refer to bundles of polyethylene chains in *trans*-planar conformation since similar results are obtained when copolymer chains are considered. The calculated X-ray scattering intensities I on the equator ($l = 0$) and on the second layer line for models with a perfect hexagonal arrangement as far as the positions of their axes are strictly similar, whatever the relative orientation of the chains. According to the theoretical considerations of Clark and Muus,[25] indeed, on the equator and the layer line with l even only the 0th order Bessel function makes appreciable contribution when 2/1 helices are considered. On the contrary, the calculated diffraction profiles on the first layer line, shown in Figure 5, are largely different, and on the basis of a comparison with the experimental diffraction profile (Figure 2B) a discrimination between the limiting ordered models can be attempted. In particular, in the pattern of the orthorhombic-like model (Figure 5A) the main peak is split in two peaks (at $\xi = 0.20$ Å^{-1} and at $\xi = 0.23$ Å^{-1}), and three less intense peaks are centered at $\xi = 0.31$ Å^{-1}, $\xi = 0.40$ Å^{-1}, and $\xi = 0.46$ Å^{-1}. In the pattern of the monoclinic-like model (Figure 5B), the most intense peak is located at 0.23 Å^{-1} and there are two weaker peaks at $\xi = 0.40$ Å^{-1} and $\xi = 0.46$ Å^{-1}. In the pattern of the triclinic-like model (Figure 5C), the most intense peak is located at $\xi = 0.21$ Å^{-1}, two intense peaks correspond to $\xi = 0.31$ Å^{-1} and $\xi = 0.43$ Å^{-1}, and a weaker peak is located at $\xi = 0.12$ Å^{-1}. We recall that

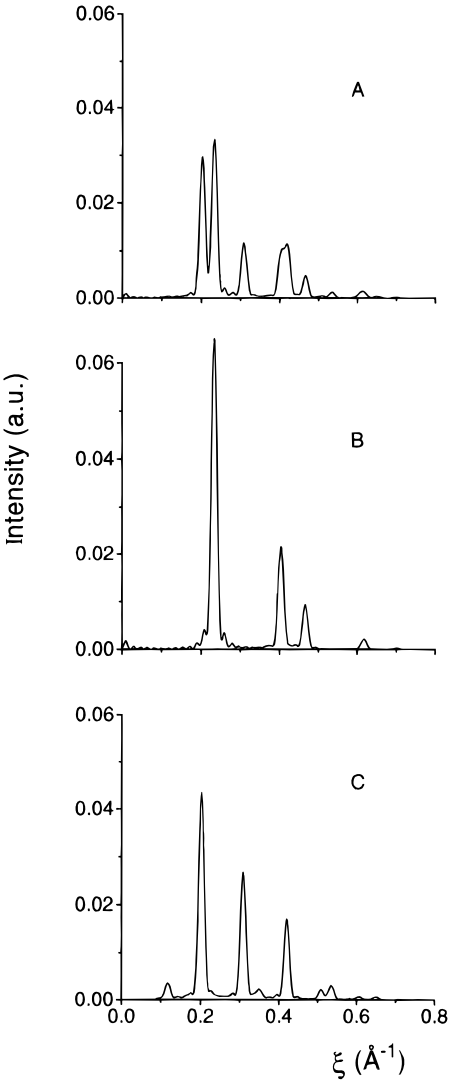

Figure 5. Calculated X-ray diffraction profiles (I) for the three limiting model structures for the first layer line. $B_\xi = 22$ Å^2, $u_\xi^2 = 0$. (A) orthorhombic-like; (B) monoclinic-like; (C) triclinic-like.

the experimental profile on the first layer line shows the presence of two broad peaks, located at $\xi = 0.23$ Å^{-1} and at $\xi = 0.43$ Å^{-1} in the intensity ratio 3:1. All the features of the pattern of Figure 5C, for the triclinic-like model, are too far from those of the experimental pattern of Figure 2B. Hence the triclinic-like model is clearly unsuitable as limiting ordered model to describe the pseudo-hexagonal form of ethylene−propylene copolymers. For this reason, the monoclinic-like as well as the orthorhombic-like arrangements of the chains (Figures 4A and 4B) seem more suitable as starting model structures in which, as will be shown in the following, one or more kinds of disorder (conformational, translational, rotational, and stacking faults) are introduced.

6.2. Conformational Disorder. For all the considered limiting ordered models, the ratio between the integrated intensity of the main peaks on the first layer line and on the equator ($(I(1)/I(0)$ nearly equal to 0.1

$$\mathbf{Q} = \begin{vmatrix} p_m \exp(-\mathbf{s_1}\cdot\mathbf{q}) & p_o \exp(-\mathbf{s_1}\cdot\mathbf{q}) & p_{tt} \exp[-(\mathbf{s_1}+\mathbf{s_2})\cdot\mathbf{q}] & p_{tt} \exp[-(\mathbf{s_1}+\mathbf{s_2})\cdot\mathbf{q}] \\ p_o \exp(-\mathbf{s_1}\cdot\mathbf{q}) & p_m \exp(-\mathbf{s_1}\cdot\mathbf{q}) & p_{tt} \exp[-(\mathbf{s_1}+\mathbf{s_2})\cdot\mathbf{q}] & p_{tt} \exp[-(\mathbf{s_1}+\mathbf{s_2})\cdot\mathbf{q}] \\ p'_t \exp[-(\mathbf{s_1}+\mathbf{s_2})\cdot\mathbf{q}] & p'_t \exp[-(\mathbf{s_1}+\mathbf{s_2})\cdot\mathbf{q}] & p_t \exp(-\mathbf{s_2}\cdot\mathbf{q}) & 0 \\ p'_t \exp[-(\mathbf{s_1}+\mathbf{s_2})\cdot\mathbf{q}] & p'_t \exp[-(\mathbf{s_1}+\mathbf{s_2})\cdot\mathbf{q}] & 0 & p_t \exp(-\mathbf{s_1}\cdot\mathbf{q}) \end{vmatrix} \quad (6)$$

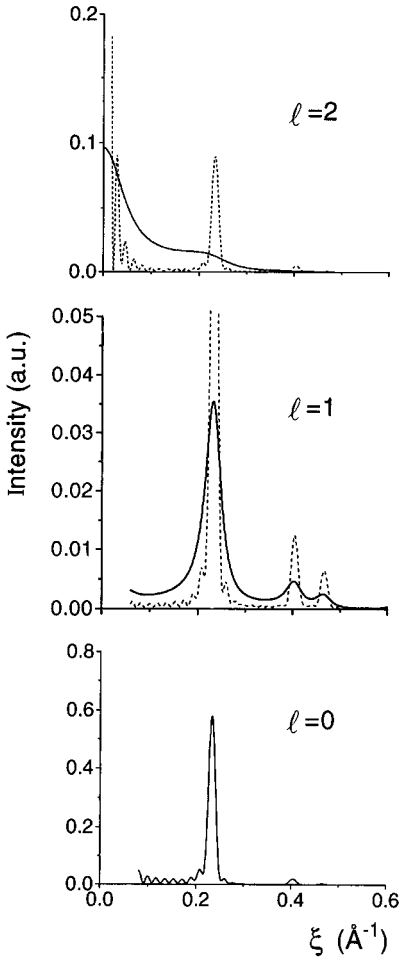

Figure 6. Calculated X-ray diffraction profiles (I) of a monoclinic-like model structure including nearly *trans*-planar chains with some conformational disorder ($\Delta = 0.5$Å, see the text, 25 mol % of propylene comonomer) for $B_\xi = 22$ Å^2, $u_\zeta^2 = 0$ (dashed lines, solid line on the equator) and $u_\zeta^2 = 0.15$ Å^2 (solid line).

for all of them) is lower than the experimental value (≈0.18). This calculated intensity ratio is slightly increased with introduction of methyl groups (for instance, $I(1)/I(0) \approx 0.13$ for 25 mol % of propylene comonomer), but it is still lower than the experimental value. $I(1)/I(0)$ may be increased upon introduction of conformational disorder, that is, some waviness in the chains implying small deviations of the dihedral angles from strictly 180° and of the valence angles from 112°. For instance, the experimental ratio $I(1)/I(0)$ may be reproduced if the average amplitude of the wave is $\Delta =$ 0.5 Å (25 mol % of propylene comonomer). This implies deviations of the dihedral and valence angles values smaller than ±20° and ±2°, respectively, and substantially unaltered mean chain periodicity. The presence of the conformational disorder in the pseudo-hexagonal form of ethylene−propylene copolymers is not surprising, being a consequence of the constitutional disorder and of the inclusion of the methyl groups in the crystalline regions.

Figure 6 plots the calculated diffraction profile for the layer lines with $0 \le l \le 2$ (dashed lines, solid line for the equator) for a model structure with all parallel chains conformationally disordered ($\Delta = 0.5$ Å, 25 mol % of propylene comonomer), as an example. It is worth noting that all the nonequatorial peaks are too narrow with respect to the experimental ones. To broaden these peaks, different kinds of disorder should be added. In particular, in the following, the influence of translational disorder along c, of rotational intermolecular disorder, and of stacking faults is investigated.

6.3. Further Kinds of Disorder. i. Translational Disorder. The effect of translational disorder on the diffraction intensities calculated for our model structures can be studied in different ways, for instance, by introducing a thermal factor along ζ (B_ζ) or paracrystalline disorder through the mean square displacement of the centers of gravity of the chains along z (u_ζ^2 in eq 1). We have preferred to use the latter factor rather than B_ζ, since u_ζ^2 broadens along ξ all the nonequatorial reflections. As already discussed before, this factor, indeed, decreases the correlation between the relative heights of the chains the more, the higher is their distance in the $x-y$ plane.

Figure 6 plots the calculated profiles on the nonequatorial layer lines for $u_\zeta^2 = 0.15$ Å^2 (solid lines) for a model structure with all parallel chains conformationally disordered ($\Delta = 0.5$ Å, 25 mol % of propylene comonomer), as an example. The equatorial profile remains unchanged upon introduction of disorder along z. The half-height width of the main peak on the first layer as well as of the meridional peak on the second layer line along ξ increases from 0.02 to 0.05 Å^{-1} ($w(1)$) and to 0.11 Å^{-1} ($w(2)$) when u_ζ^2 increases from zero to 0.15 Å^2. The paracrystalline translational disorder along z leaves nearly unaltered the ratio $I(1)/I(0)$ and influences strongly the ratio $I(2)/I(0)$ (for instance $I(2)/I(0)$ decreases from 7 to 1 with increasing u_ζ^2 to 0.15 Å^2).

ii. Rotational Disorder. The effect on the intensities of intermolecular rotational paracrystalline disorder, as described by Hosemann[21] and indicated by Tadokoro in ref 22 as disorder of second kind, has been considered. We report calculations for random rotations of the chains around their axes, of an angle comprised in the range $\pm|\omega|$, starting from their ideal position. In these models, the loss of correlation in the angular orientation between the chains with respect to their starting position increases with increasing their distance; as a result, the long-range order is lost, but a short-range order remains between each chain and its nearest neighbors. The effect of this kind of disorder is reported here for the model structures with chains in the *trans*-planar conformation and in a monoclinic-like arrangement. Since this kind of disorder can influence only the diffraction profiles on the layer lines with odd l values for ensembles of 2/1 helices,[25] only the diffraction on the first layer line is reported for different values $|\omega|$ of the maximum angular displacement between adjacent chains in Figure 7. This kind of disorder does not broaden the peaks but produces diffuse scattering in the background.

iii. Disorder in the Piling of Layers of Chains, Stacked with Faults. Introducing stacking faults, as described previously (using method II), mainly influences the first layer line. In these calculations the polymer chains have been assumed to be correlated as far as their reciprocal orientation and the relative heights along z only locally, while after three or four unit cells this correlation is almost completely lost. If so, the diffraction of the nonequatorial layer lines may be approximated, at least as far as the Bragg contribution, by the diffraction of a small bundle of few chains, the interference among these bundles, producing only a background.[22] We further suppose that, inside these smaller aggregates of chains, stacking faults may occur.

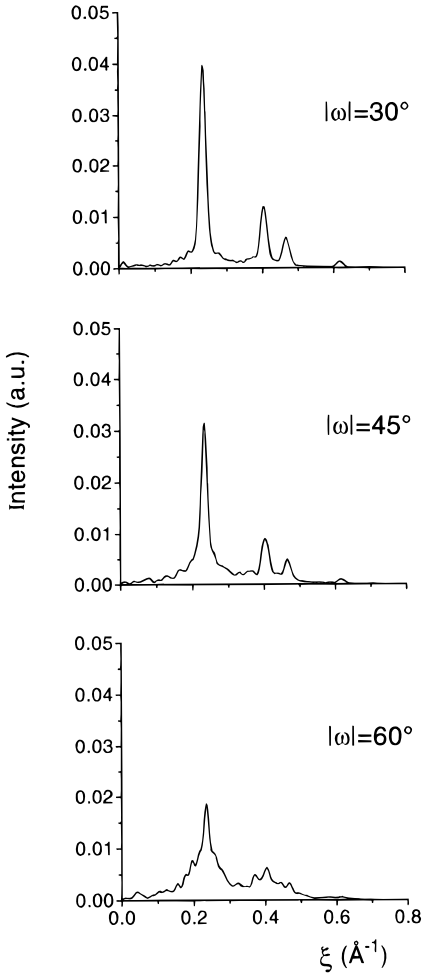

Figure 7. Calculated X-ray diffraction profiles (I) on the first layer line (l = 1) of the monoclinic-like model structure in which adjacent chains are rotated around their axis by an angle comprised in the range $\pm\omega$. B_ξ = 22 Å^2.

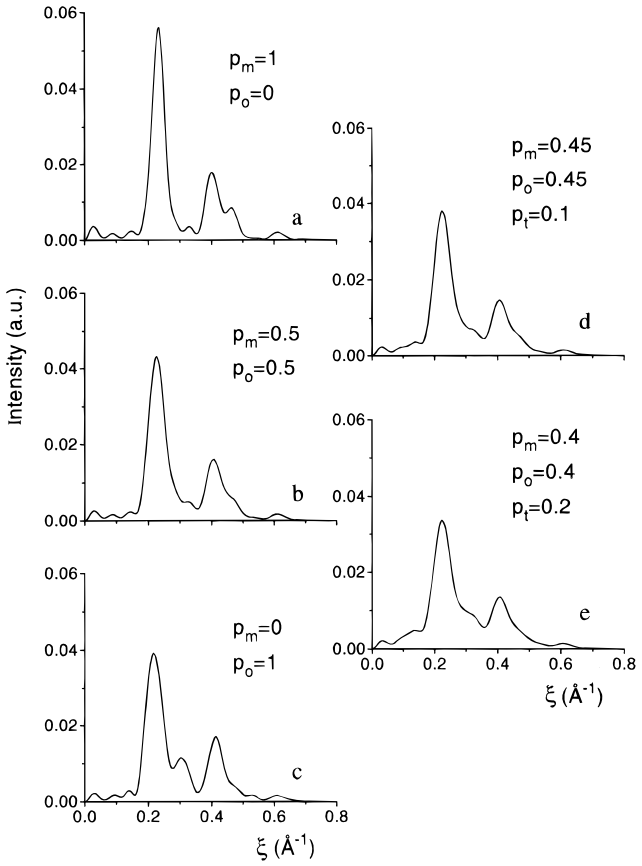

Figure 8. Calculated X-ray diffraction profiles (I) on the first layer line (l = 1) for bundles of 16 chains including stacking faults (see text) (4 layers, 4 chains each). (a) p_m = 1, p_o = 0, p_t = 0; (b) p_m = 0.5, p_o = 0.5, p_t = 0; (c) p_m = 0, p_o = 1, p_t = 0; (d) p_m = p_o = 0.45, p_t = 0.10; (e) p_m = p_o = 0.40, p_t = 0.20. B_ξ = 22 Å^2.

Figure 8 plots the calculated diffraction intensities along the first layer line for bundles comprising four layers, each layer made up of four chains, for p_m = 1, p_o = 0, p_t = 0 (curve a); p_m = 0.5, p_o = 0.5, p_t = 0 (curve b); p_m = 0, p_o = 1, p_t = 0 (curve c); p_m = p_o = 0.45, p_t = 0.1 (curve d); p_m = p_o = 0.40, p_t = 0.20 (curve e), as an example. From the pattern of Figure 8 it is apparent that, if the size of the correlated zones is small, the experimental broadness of the main peak on the first layer line may be easily accounted for. However, a short-range order has to be maintained corresponding to the relative shifts of neighboring chain, nearer to those observed in the monoclinic-like and orthorhombic-like models, and to a lesser extent as in the triclinic-like model.

7. Discussion and Conclusive Remarks

A detailed X-ray diffraction pattern of an oriented sample of the ethylene−propylene copolymer (75 mol % of ethylene) in the pseudo-hexagonal form has been presented. This pattern confirms some structural features anticipated by previous studies:[1]

- the positions of the three narrow equatorial diffraction peaks indicate an ordered hexagonal arrangement of the chain axes (a = 4.94 Å);

- the well-defined layer lines indicate the nearly *trans*-planar conformation of the chains (c = 2.54 Å);

- the broadness of all the nonequatorial peaks indicates the occurrence of some packing disorder.

The semiquantitative comparison between the experimental diffraction intensities with the calculated intensities for ordered and disordered pseudo-hexagonal chain aggregates has allowed us to clarify some additional features of the structure of the pseudo-hexagonal form of the ethylene−propylene copolymers:

(i) the long-range order only occurs with respect to the parallelism, the lateral spacing among the chain axes, and the single chain periodicity along the chain axes; the order in the relative angular orientation and the relative axial positions along z is far less extensive;

(ii) a short-range order in the packing of nearly *trans*-planar copolymer chains corresponds locally to relative shifts of neighboring chains (having nearly the same quote along z) nearer to those observed in the monoclinic and in the more common orthorhombic form of polyethylene;

(iii) the methyl groups of the propylene monomeric units are included in the crystalline phase. In fact, the chains in the crystals have lengths of the order of 30 monomeric units while the fraction of ethylene sequences exceeding this length is negligible for copolymer with a 75 mol % ethylene content. The presence of methyl groups in the crystals is associated with conformational and packing disorder;

(iv) the ratio between the integrated intensities of the main peaks on the first layer line and on the equator can be accounted for only by conformational disorder, implying, for instance, a waviness of the nearly *trans*-planar chains and small deviations from 180° of internal rotation angles in the chain backbone;

(v) some further partial disorder (intermolecular translational along *c* and intermolecular rotational around *c*) should be introduced to account for the broadness of the nonequatorial peaks.

Let us conclude with a comparison between the present proposed structure for the pseudo-hexagonal form of the ethylene−propylene copolymer with other disordered structures, also presenting a hexagonal arrangement of the chain axes, as far as conformational and intermolecular (packing) disorder.

Disordered pseudo-hexagonal crystalline forms have been described for several homopolymers, for instance, for atactic polyacrilonitrile (PAN) in the most common polymorphic form[26] and poly(tetrafluoroethylene) (PTFE) in the high temperature forms (IV and I)[16] and polyethylene, in the polymorph stable at high temperature and pressure.[27] Disordered pseudo-hexagonal forms are also common for copolymers like, for instance, the alternated ethylene−tetrafluoroethylene copolymers (ETFE) in the high temperature form[17] and the random tetrafluoroethylene−hexafluoropropene copolymer (FEP) in the high temperature form.[28]

As far as the conformational disorder is concerned, it is particularly large for the configurationally disordered PAN chains as well as for the high pressure form of polyethylene. In both cases, the mean chain periodicity is shorter (≈2.4 Å) than 2.54 Å, corresponding to the presence of *gauche* conformations besides *trans*.[26,27] The conformational disorder would be lower for the high temperature (above 30 °C) form I of PTFE, corresponding to the occurrence of reversals between left- and right-handed helical structures presenting backbone dihedral angles all equal to +165° or −165°.[16] For the high temperature form of ETFE,[17] the conformational disorder corresponds to small deviations from the *trans*-planar conformation, the mean chain periodicity for two carbon atoms being close to 2.52 Å. The conformational disorder would be substantially absent for the 15/7 helix of the form IV of PTFE (stable between 19 and 30 °C).[16] Hence, as far as the chain conformation, the structure of the pseudo-hexagonal form of the ethylene−propylene copolymers would be close to that proposed for the high temperature form of ETFE.

As far as the intermolecular disorder is concerned, nearly complete translational (along *c*) and rotational (around *c*) disorder is present in the PAN pseudo-hexagonal form as well as in the high temperature form of ETFE. A nearly complete rotational disorder, associated with a short-range translational (along *c*) order (which, however, is lost for temperatures above 150 °C), would be present in form I of PTFE. Only small rotational (around *c*) and translational (along *c*) displacements of the 15/7 helices with respect to an ordered structure would be present in phase IV of PTFE. In particular, the short-range translational order would consist of the positioning of the carbon atoms of neighboring chains nearly at the same height. Hence, as far as the intermolecular disorder is concerned, the latter structure would be close to that proposed for the pseudo-hexagonal form of the ethylene−propylene copolymers (see paragraph ii of this section). The similarity is also related to the positioning along *c* of the chains. In fact, in both structures there would be short-range order involving neighboring chains having nearly the same quote along *z*.

Acknowledgment. The authors thank dr. Maurizio Galimberti and dr. Enrico Albizzati of Montell "Centro Ricerca Giulio Natta" of Ferrara for useful discussions and for providing the examined samples. This work was supported by the Ministero dell' Università e della Ricerca Scientifica e Tecnologica (Italy), by Consiglio Nazionale delle Ricerche, and by Montell Polyolefins. X-ray diffraction data were recorded with a Nonius CAD4 automatic diffractometer (Centro Interdipartimentale di Metodologie Chimico Fisiche, University of Naples).

References and Notes

(1) Bassi, I. W.; Corradini, P.; Fagherazzi, G.; Valvassori A. *Eur. Polym. J.* **1970**, *6*, 709.

(2) Ver Strate, G.; Wilchinsky, Z. W. *J. Polym. Sci., Part A-2*, **1971**, *9*, 127.

(3) Baldwin, F. P.; Ver Strate, G. *Rubber Chem. Technol.* **1972**, *45*, 709.

(4) Guerra, G.; Ilavský, M.; Biroš, J.; Dušek, K. *Colloid Polym. Sci.* **1981**, *259*, 1190.

(5) Scholtens, B. J. R.; Riande, E.; Mark J. E. *J. Polym. Sci., Polym. Phys. Ed.* **1984**, 22, *1223*.

(6) Walter, E. R.; Reding E. P. *J. Polym. Sci.* **1956**, *21*, 561.

(7) Cole, E. A.; Holmes D. R. *J. Polym. Sci.* **1960**, *46*, 245.

(8) Swann, P. R. *J. Polym. Sci.* **1962**, *56*, 409.

(9) Wunderlich, B.; Poland, D. *J. Polym. Sci., Part A* **1963**, *1*, 357.

(10) Baker, C. H.; Mandelkern, L. *Polymer* **1965**, *7*, 71.

(11) Crespi, G.; Valvassori, A.; Zamboni, V.; Flisi, U. *Chim. Ind. (Milan)* **1973**, *55*, 130.

(12) Preedy, J. E. *Br. Polym. J.* **1973**, *5*, 13.

(13) Bunn, C. W. *Trans. Faraday Soc.* **1939**, *35*, 482.

(14) Corradini, P.; Guerra, G. *Adv. Polym. Sci.* **1992**, *100*, 183.

(15) Tritto, I.; Fan, Z.-Q.; Locatelli, P.; Sacchi, M. C.; Camurati, I.; Galimberti, M. *Macromolecules* **1995**, *28*, 3342.

(16) a) Bunn, C. W.; Howells, E. R. *Nature (London)* **1954**, *174*, 549. (b) Clark, E. S.; Muus, L. T. *Z. Kristallogr.* **1962**, *117*, 119. (c) Corradini, P.; De Rosa, C.; Guerra, G.; Petraccone V. *Macromolecules* **1987**, *20*, 3043. (d) De Rosa, C.; Guerra, G.; Petraccone, V.; Centore, R.; Corradini, P. *Macromolecules* **1988**, *21*, 1174. (e) Kimmig, M.; Strobl, G.; Sthühn, B. *Macromolecules* **1994**, *27*, 2481.

(17) (a) Tanigami, T.; Yamamura, K.; Matsuzawa, S.; Ishikawa, M.; Mizoguchi, K.; Miyasaka, K. *Polymer* **1986**, *27*, 1521. (b) Iuliano, M.; De Rosa, C.; Guerra, G.; Petraccone, V.; Corradini, P. *Makromol. Chem.* **1989**, *190*, 827. (c) D'Aniello, C.; De Rosa, C.; Guerra, G.; Petraccone, V.; Corradini, P.; Ajroldi, G. *Polymer* **1995**, *36*, 967.

(18) Seto, T.; Hara, T.; Tanaka, K. *Jpn. J. Appl. Phys.* **1968**, *37*, 31.

(19) Muller, A.; Lonsdale, K. *Acta Crystallogr.* **1948**, *1*, 129.

(20) Kitaigorodsky, A. I. *Organicheskaya Kristallokhimiya*; Press of the Acad. Sci. USSR: Moskow; Revised English translation, Consultants Bureau: New York, 1961.

(21) Hosemann, R.; Bagchi, S. N. *Direct Analysis of Diffraction by Matter*; North-Holland Publishing Co.: Amsterdam, 1962.

(22) Tadokoro, H. *Structure of Crystalline Polymers*; Wiley: New York, 1979.

(23) Auriemma, F.; Petraccone, V.; Dal Poggetto, F.; De Rosa, C.; Guerra, G.; Manfredi, C.; Corradini, P. *Macromolecules* **1993**, *26*, 3772.

(24) Allegra, G. *Nuovo Cimento* **1962**, *23*, 502.

(25) Clark, E. S.; Muus, L. T. *Z. Kristallogr.* **1962**, *117*, 108.

(26) (a) Lindenmeyer, P. H.; Hosemann, R. *J. Appl. Phys.* **1963**, *34*, 42. (b) Liu, X. D.; Ruland, W. *Macromolecules* **1993**, *26*, 3030. (c) Rizzo, P.; Auriemma, F.; Guerra, G.; Petraccone, V.; Corradini, P. Submitted to *Macromolecules*.

(27) (a) Bassett, D. C.; Block, S.; Piermarini, G. J. *J. Appl. Phys.* **1974**, *45*, 4146. (b) Yamamoto, T. *J. Macromol. Sci., Phys.* **1979**, *B16*, 487.

(28) Weeks, J. J.; Eby, R. R.; Clark, E. S. *Polymer* **1981**, *22*, 1496.

MA960511Z